ELSEVIER

Journal of Structural Geology 28 (2006) 185–199

JOURNAL OF STRUCTURAL GEOLOGY

www.elsevier.com/locate/jsg

Structural evolution of a fold and thrust belt generated by multiple décollements: analogue models and natural examples from the Northern Apennines (Italy)

Donatella Massoli [a,*], Hemin A. Koyi [b], Massimiliano R. Barchi [a]

[a] *Department of Earth Sciences, University of Perugia, Italy*
[b] *Hans Ramberg Tectonic Laboratory, Department of Earth Sciences, Uppsala University, Sweden*

Received 7 November 2005; accepted 8 November 2005
Available online 6 January 2006

Abstract

This study analyses the role played by the mechanical proprieties of the rocks involved in a thrust system, focusing on the problem of multiple décollements and of related compressional structures. Integration of geophysical (seismic reflection profiles) and geological data and scaled sandbox models are used to study the deformation style of two areas of the Northern Apennines (Italy): the Po Plain and the Umbria-Marche Apennines. Both areas are characterised by a complex stratigraphy, consisting of décollements located at different depths that influence the geometry and kinematics of the thrust system. The main characteristic of the models presented here is the presence of two décollement horizons, situated at the base and in an intermediate level of the models. During deformation of the models, these two décollement horizons generate two sets of structures, with different geometrical characteristics and significance. Through the joint analysis of geophysical and geological data and model results, wavelengths of the compressional structures analysed show that the structural style of the two analysed areas is almost similar. Moreover, model results prove that the final configuration of the thrust system follows the general rules of evolution of a wedge deformed above a weak décollement and is largely governed by the larger, deep seated structures.

Keywords: Multiple décollements; Sand-box models; Seismic reflection profiles; Northern Apennines of Italy

1. Introduction

The structural evolution of a thrust system depends on stratigraphy, mechanical property of the rocks, duration and rate of deformation and uplift versus subsidence ratios (Chester et al., 1991; Fischer and Woodward, 1992; Marshak and Wilkerson, 1992; Doglioni and Prosser, 1997). In particular, the mechanical property of the deformed rocks (e.g. presence of competence contrasts) and the décollement appear to be of great significance in influencing the final geometry of the structures and the kinematics of the thrust system (Davis and Engelder, 1985; Letouzey et al., 1995; Sans and Vergés, 1995; Teixell and Koyi, 2003; Koyi et al., 2003).

Some studies on thrust systems have paid particular attention to the style of thrusting, changes in fault attitude, displacement rate and amount and ramp angle (Dahlstrom, 1970; Elliott, 1976; Berger and Johnson, 1980; Mitra, 1986; Eisenstadt and De Paor, 1987; Fermor and Moffat, 1992). Other studies have instead focussed on the role of rheology of the basal décollement, showing how markedly different wedges develop above a ductile or a frictional layer, respectively (Davis and Engelder, 1985; Baker et al., 1988; Cello and Nur, 1988; Cobbold et al., 1989; Letouzey et al., 1995; Gutscher et al., 1996; Teixell, 1996; Cotton and Koyi, 2000; Leturmy et al., 2000; Turrini et al., 2001; Costa and Vendeville, 2002; Grelaud et al., 2002; Koyi and Cotton, 2004).

The present paper aims to analyse the role of multiple décollements in the Northern Apennines fold and thrust belt (Italy), specifically considering two different areas of the belt: the Po Plain and the Umbria-Marche Apennines (Fig. 1). We study these regions by interpreting the available geophysical and geological data and by performing a set of scaled sandbox models.

In particular, our goal is to answer the following questions:

- Are multiple décollements responsible for the development of different sets of structures in this fold and thrust belt? Can these structures be easily distinguished by their geometry and wavelength?

* Corresponding author.
E-mail address: dmassoli@unipg.it (D. Massoli).

0191-8141/$ - see front matter © 2006 Elsevier Ltd. All rights reserved.
doi:10.1016/j.jsg.2005.11.002

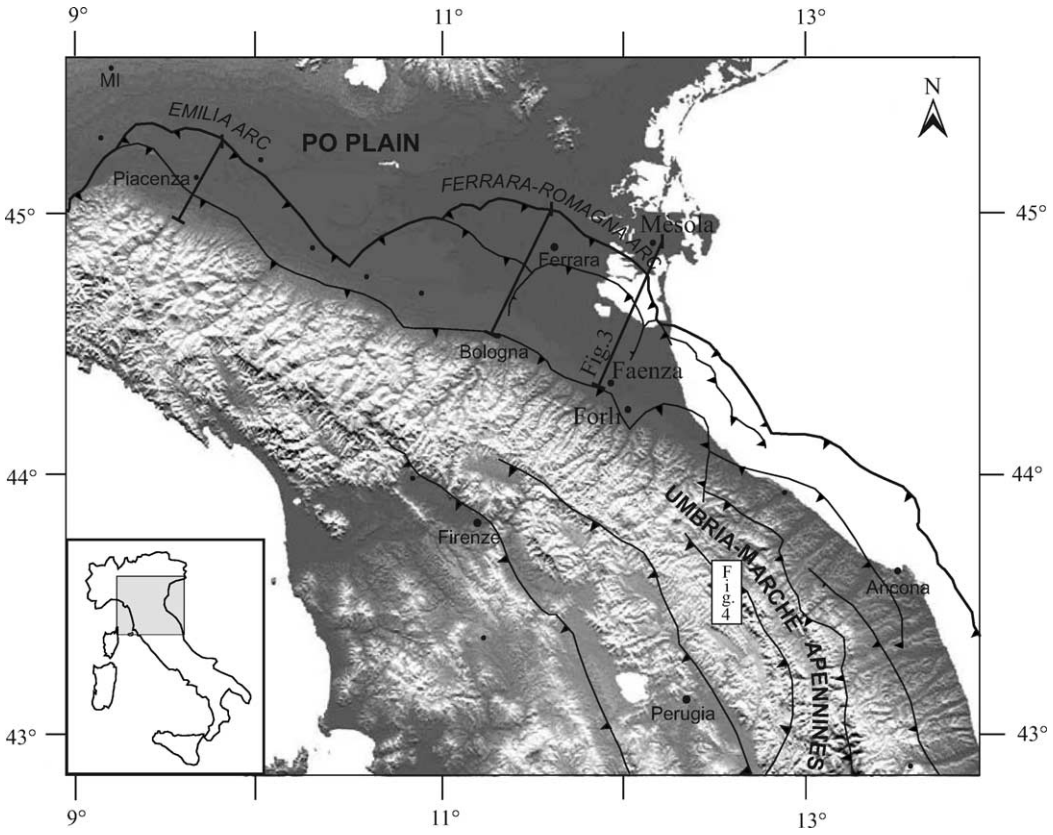

Fig. 1. Shaded relief and schematic map of the Northern Apennines fold-and-thrust belt. The black lines represent the traces of the regional seismic profiles.

- In which way does the presence of multiple décollements influence the time/space evolution of the Northern Apennines thrust belt? Can multiple décollements perturbate the regular, in-sequence nucleation of thrusting (e.g. Boyer and Elliot, 1982)?

Our set of sandbox models aim at reproducing the main features of the Po Plain (PP) and Umbria-Marche Apennines (UMA), focusing on their deformation style. The main characteristic of the sandbox models is the presence of two décollements, situated at two different stratigraphic levels. Some parameters of the models, such as thickness, final bulk shortening and lateral dimensions, have been systematically changed, in order to study their influence on the evolution and final configuration of these models.

Our study argues that the presence of multiple décollements nucleates different sets of structures with different significance and geometrical characteristics. Moreover, part of the complexity of the thrust system derives from the decoupling between deeper and shallower structures, due to the presence of the upper décollement. These results can be used to understand other fold and thrust belts possessing multiple décollements.

2. Geological framework

The PP and the UMA both belong to the external part of the Northern Apennines (NA) (Fig. 1), which is an arc-shaped fold-thrust belt, with northeastward convexity and vergence (Barchi et al., 2001 and reference therein). This belt developed prevalently in Neogene times, in the framework of the collision of the European continental margin (Sardinia–Corsica block) and the Adriatic microplate (e.g. Alvarez, 1972; Reutter et al., 1980).

The PP, located in a northernmost and structurally external position with respect to the exposed chain, is part of the NA deformed foreland, where the compressional structures are buried below a thick syntectonic succession, deposited in the Neogene–Quaternary foredeep. The present-day geological configuration of the PP is the result of the interaction of several parameters, such as amounts and rates of convergence, uplift, sedimentation and subsidence. The high value of the two latter parameters promoted the deposition of a thick clastic succession, which seals the external fronts of NA. During the late Messinian–early Pliocene time interval, the evolution of the foredeep was driven by a thrust system evolving in a piggy-back mode towards the foreland (i.e. northeastward). Thereafter, from the middle Pliocene onwards, the migration of the flexural margin of the foredeep was locked by the previously formed, opposite verging, Southern Alps structures: consequently, thrusting occurred also in an out-of-sequence mode (Castellarin, 2001). The contractional, N–S-trending stress field is still active in the PP region, as indicated by data coming from structural analyses (Perotti, 1991; Sorgi et al., 1998; Mariucci et al., 1999) as well as from geophysical studies and seismological evidence (Cagnetti et al., 1978; Boccaletti et al., 1985; Gasparini et al.,

1985; Frepoli and Amato, 1997; Anzidei et al., 2001; Selvaggi et al., 2001; Lavecchia et al., 2004).

Given the lack of exposed structures, the structural setting of the PP is essentially imaged by a dense grid of reflection seismic data collected for industrial purposes by Agip (the Italian national oil industry, presently ENI-E&P) since 1945 (Rizzini and Dondi, 1979; Pieri and Groppi, 1981; Pieri, 1983). Analysis of the seismic reflection profiles shows that the Apennines front consists of a system of three arcuate thrusts (from W to E: Monferrato, Emilia and Ferrara-Romagna arcs) (Fig. 1). These arcs generally trend WNW–ESE, (Dondi et al., 1982; Ori et al., 1986), which is in accordance with the overall northeastward transport direction of the thrust sheets in the Northern Apennines (Elter et al., 1975) (Fig. 1).

The UMA is located in an innermost and southernmost position relative to the PP: it represents the main mountain ridge of the Northern Apennines, where Mesozoic and early Tertiary carbonatic rocks extensively crop out. In this area, the geometry and kinematics of the exposed contractional structures can be analysed. The geometry at depth can be constrained by well data and seismic profiles. This classical fold-and-thrust belt developed during the middle Miocene–early Pliocene time interval: the innermost contractional structures are disrupted by subsequent extensional tectonics.

Some authors have suggested that the UMA has developed as a thin-skinned fold-thrust belt detached above a single main décollement (Triassic Evaporites), overlying an undeformed basement (Baldacci et al., 1967; Decandia and Giannini, 1977). This point of view was adopted and discussed in a very important and influential paper (Bally et al., 1986) where seismic profiles were firstly used to study the structural evolution of the UMA. Other authors have hypothesized the involvement of the basement as well (Lavecchia et al., 1987; Barchi, 1991; Sage et al., 1991). In recent years, data from the CROP 03 deep seismic reflection profile (Pialli et al., 1998) detected the involvement of the basement in the deformation more clearly (Barchi et al., 1998), confirming thick-skinned nature of the deformation.

2.1. Stratigraphy

The NA stratigraphic succession evolves from a Mesozoic–Paleogene passive margin to a Neogene–Quaternary foredeep basin (e.g. Argnani and Ricci Lucchi, 2001; Barchi et al., 2001). The former is characterised bottom to top by shallow marine evaporitic, carbonate platform and pelagic carbonate basin successions, whereas the latter by syntectonic, mostly turbiditic sediments.

The Mesozoic–Paleogene passive margin succession (e.g. Centamore et al., 1986; Cresta et al., 1989; Passeri, 1994) is exposed in the UMA and can be subdivided into four main lithological groups, each characterized by formations having similar competence, internal stratigraphy, and seismic expression. This subdivision allows us to consider each group as a distinct element with a specific mechanical behaviour under the tectonic deformation. The groups are, from bottom to top: (1) Palaeozoic phyllitic basement; (2) Triassic evaporitic group (i.e. alternated anhydrites and dolomites); (3) Jurassic–Cretaceous carbonatic group; and (4) Paleogene marly group (Fig. 2).

The Mesozoic–Paleogene stratigraphy of the PP is essentially the same as that of the UMA, but this succession

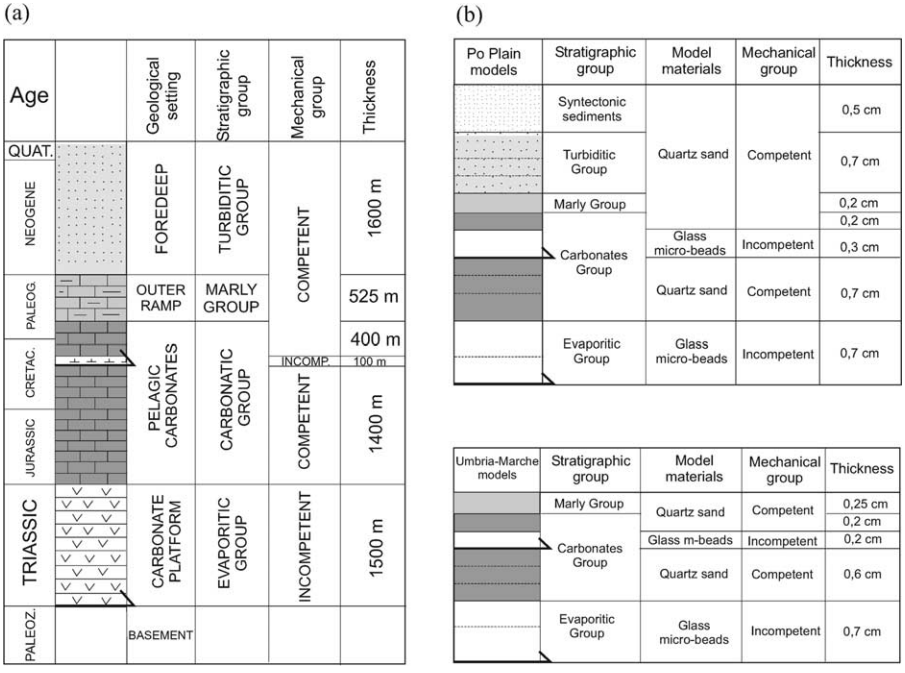

Fig. 2. (a) Schematic regional and mechanical stratigraphy of the Northern Apennines fold-and-thrust belt. The arrows indicate the shallower (Marne a Fucoidi Fm.) and the deeper (Triassic evaporites) main décollement levels. The reported thickness represents average values. (b) Stratigraphy of Po Plain models and Umbria–Marche models and corresponding parameters of modelling materials.

is covered by a thick wedge of Neogene–Quaternary syntectonic sediments, consisting of marls, turbidites and marine clays and sands. These sediments are sourced from both the Alpine and Apennine chains, and evolve through time from deep marine to shallow marine and eventually to continental units (e.g. Argnani et al., 1997). They can be easily subdivided into packages separated by either non-depositional erosional or angular unconformities, related to both eustatic variations and synsedimentary tectonic activity (i.e. development of blind thrusts and associated folds). The clastic succession is also characterised by dramatic lateral changes in thickness and facies, in contrast with the regular, almost tabular shape of the underlying, passive margin sequences.

From a mechanical point of view, the NA stratigraphy can be considered as composed by alternating competent and not-competent units (Fig. 2). Two major décollements influence the regional structural setting: the basal décollement (Triassic evaporites), located at the bottom of the Mesozoic succession, decouples the sedimentary cover from the underlying basement; the upper décollement (Marne a Fucoidi formation (MF)), localised just below the Mesozoic–Tertiary boundary, decouples the clastic syntectonic succession from the underlying passive margin sequence (Baldacci et al., 1967; Pieri and Groppi, 1981; Castellarin et al., 1985; De Feyter, 1989; Barchi et al., 1998). Many other, minor décollements are present, mainly corresponding to marly horizons, interlayered within both the carbonates and the turbidites.

3. Structural style

The structural style of the NA is strongly influenced by the mechanical anisotropy in the stratigraphy. Different sets of structures that generated at different structural levels linked to each other and developed in a hierarchical mode, can be distinguished. In particular, it can be observed that each set of structures is related to a characteristic décollement and that the dimension of the structures is proportional to the depth of the décollement that they sole to: the deeper the décollement, the larger the structures (Barchi et al., 1998; Grandinetti et al., 2000).

The presence of multiple décollements in the NA is supported by both field observations (e.g. Koopman, 1983; De Feyter, 1989) and interpretation of seismic reflection profiles (Pieri and Groppi, 1981; Castellarin et al., 1985; Bally et al., 1986; Barchi et al., 1998; Pauselli et al., 2002).

The current research focuses on two types of structures, related to two major décollements:

(1) deep-seated (large) structures, involving the entire sedimentary cover above the Triassic evaporites, which constitute the basal décollement level;
(2) shallow-seated (small) structures, detached above the MF and involving only the upper part of the succession (i.e. marly and turbiditic groups).

In order to compare the structural style of the PP and UMA areas, we analysed regional seismic reflection profiles across the PP, showing the geometry of the buried compressional structures, and a set of geological sections across the UMA, where the structures involving the Jurassic–Paleogene carbonates are exposed and can be easily mapped in the field.

3.1. Seismic reflection profiles

The quality of the available commercial seismic data is good enough for description of the geometry of the deep structures and the reconstruction of the deformation history in the PP. Within this dataset, three regional seismic lines across the Emilia and the Ferrara-Romagna Fold Arcs (see Fig. 1 for location) have been interpreted and studied in detail. The interpretation has been calibrated with numerous boreholes and took into account the observations of a network of closely spaced cross and tie lines. Borehole data enabled the stratigraphic control of the seismic horizons, which constituted the base for our seismic interpretation. Only one of these seismic lines is shown here (Fig. 3).

The main seismic markers, which can be traced throughout the investigated area, are located within the turbiditic and carbonatic groups. From top to bottom they are: top Pliocene (P2); top early Pliocene (P1); top Messinian (M); top early Messinian (lowM); and Marne a Fucoidi formation (MF) (Fig. 3).

The MF marker is a Cretaceous marly formation, located close to the top of the carbonates (Fig. 2), and represents a very good stratigraphic marker with respect to both the overlying and underlying limestone formations. Due to its lateral continuity and facies uniformity, this marker has been commonly used in seismic interpretation also for the adjacent areas of the NA (Bally et al., 1986; Barchi et al., 1998). The other marker horizons represent boundaries between sedimentary cycles, within the Neogene syntectonic sediments.

Broad variations in facies, thickness, sedimentation and subsidence rates reflect different tectonic histories, which affected adjacent portions of the belt, underlying the strict connection between the local geometry and kinematics of thrusting and the evolution of the corresponding turbiditic basin (Ricci Lucchi et al., 1982; Ori et al., 1991).

At a regional scale, the analysis of the seismic profiles confirms the previous knowledge about the evolution of the thrust belt, in particular:

(a) the progressive nucleation of the compressional structures towards the foreland, suggesting an in-sequence evolution of the thrust-system (from south to north), and a contemporaneous, along-strike migration of the deformation from the western to the eastern arcs (Castellarin et al., 1985);
(b) the increase of shortening from NW to SE, in accordance with the anticlockwise rotation of the Italian peninsula (Channel et al., 1979).

Even if the structures are not cylindrical, the overall structural setting, resulting from the analysis of the three

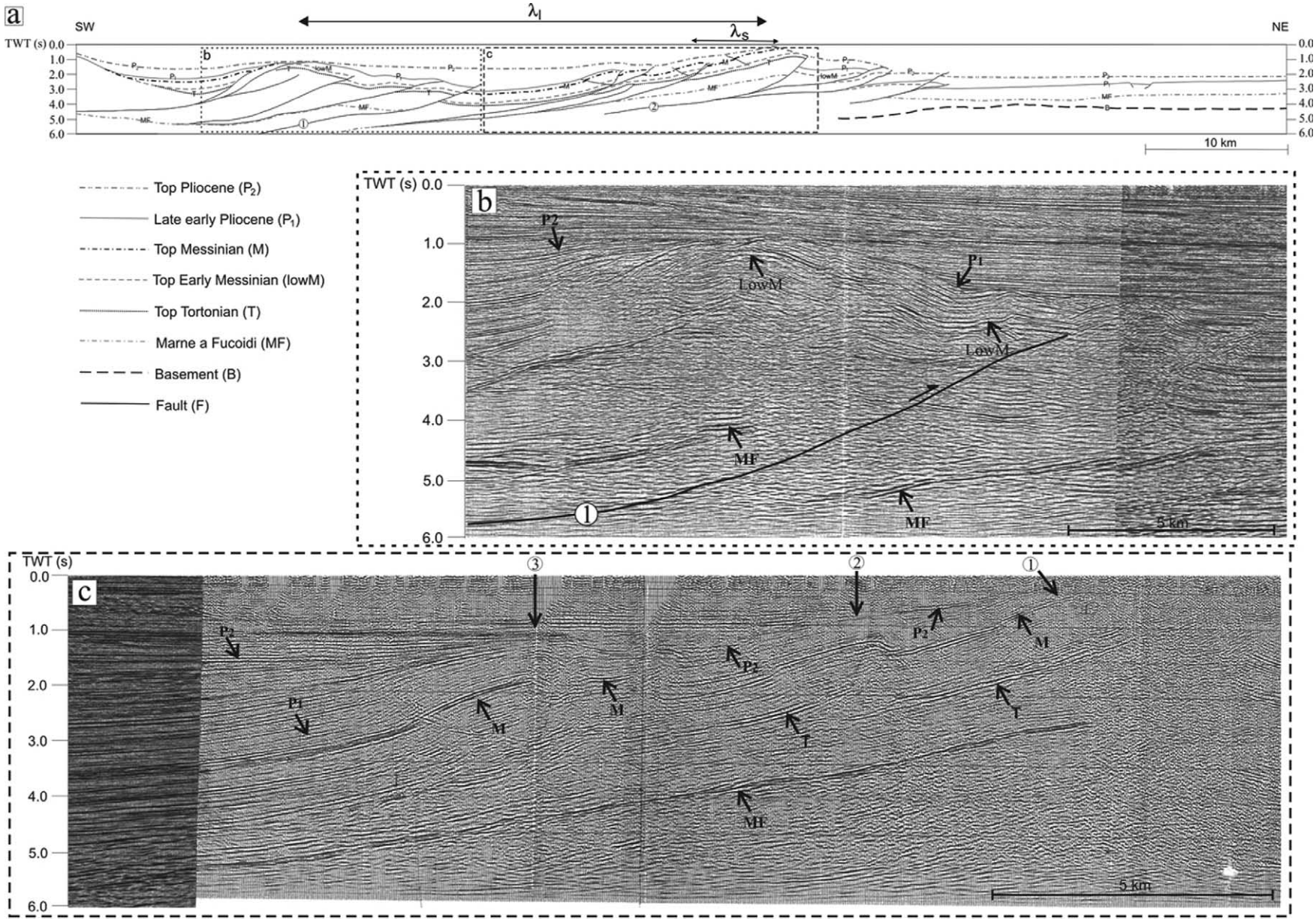

Fig. 3. (a) Line drawing of the seismic profile across the eastern part of the Ferrara–Romagna arc (see Fig. 1 for location). λ_l: wavelength of the large structures; λ_s: wavelength of the small structures; 1 and 2: major thrusts generating long-wavelength structures. (b) Seismic line of box b in (a) showing the involvement of the carbonates in the deformation (dislocation of the MF reflector). (c) Seismic line of box c in (a) showing a set of small structures (1–3) detached above the upper décollement level (MF Fm.).

regional profiles considered in this study, is quite similar: only minor variations occur in the structural style, along with a progressive increase of the shortening from west to east.

Analysis of the relationships between the growth strata and the structures constrains the timing of deformation, which is concentrated in the upper Messinian–Pliocene time interval. In particular, in this sector of the PP two major pulses of compressional deformation occurred during the lower and the upper Pliocene. The deformation continued at least until the lower Pleistocene, whilst present-day activity is debated (Di Bucci and Mazzoli, 2002; Benedetti et al., 2003; Burrato et al., 2003).

Here we describe the easternmost of the three regional profiles, being the more representative of the deformation style of the region (Fig. 3). The profile crosses the eastern part of the Romagna-Ferrara Folds, it starts near the town of Faenza and finishes near the Mèsola village, in proximity of the Po River. It is 85 km long, oriented SW–NE, and reaches a depth of 6 s (TWT), corresponding to about 10 km of depth.

A line drawing of the regional seismic profile (Fig. 3a) and two sections of the original seismic data (Fig. 3b and c) show the detailed structural configuration. In the regional view, two major thrusts (deep-seated structures, generating long-wavelength folds), involving the carbonates, occur along the section (Fig. 3a). They separate areas where syntectonic sediments reach their maximum thickness (up to 5500 m). From each major thrust, an imbricate system splays out towards the foreland (i.e. toward the north), generating a set of small (short wavelength) folds, involving only the Neogene turbidites (Fig. 3c). The seismic profile also shows the presence of many other activated décollements, producing further, local complexity: these latter minor structures do not significantly affect the regional setting and are not discussed in this study.

The relationships between shallow and deep seated thrusts are well imaged by this seismic profile. In the central part of the profile (Fig. 3a and c), the main feature is the structural disharmony of the clastic Neogene–Quaternary succession with respect to the deeper folds involving the Mesozoic carbonates. A set of three, north-verging, relatively small detachment anticlines, involving only the Neogene turbidites (from lowM to P2), is detected above the top of the carbonates. The underlying MF reflector is not involved in these thrusts but acts as a décollement, and regularly dips towards the hinterland. Moving to the southernmost and deeper part of the section (Fig. 3a and b), the innermost, large anticline is shown, generated by a deep-seated thrust, displacing the MF reflector and involving the whole carbonates succession in its hanging wall. Unfortunately, the structurally complex zone, where the doubling of the carbonates succession occurs, is not fully imaged by this seismic profile. However, in the hanging wall block, the MF reflector is structurally about 1 s higher than in the footwall block, and the offset can be easily linked to the easternmost splays. Summarising, a single, major thrust displaces the carbonates in the innermost part of the section, and then propagates northward with a flat trajectory, above the MF reflector, generating an imbricated thrust system in its hanging wall. This profile shows that the shallow-seated structures represent an imbricated thrust system, splaying out from the innermost, deep-seated major thrust.

The quality and acquisition depth of the seismic profiles through the PP are not sufficient to constrain, in a reliable way, the geometry and depth of the décollement of the deep-seated structures, which are generally supposed to be detached within the Triassic evaporites (e.g. Castellarin et al., 1985).

In order to quantitatively characterise the observed structures, and to compare them with the results of the analogue models, we measured the wavelengths (i.e. distance between the axial plane traces of two adjacent anticlines) of both the deep-seated (λ_l) and the shallow-seated (λ_s) structures, as illustrated in Fig. 3a. We collected these data along the three studied seismic profiles, as well as along other published profiles across the Po Plain region (Pieri and Groppi, 1981; Castellarin et al., 1985). The wavelength of the deep-seated structures range between ~16 and 33 km, whereas the wavelength of the shallow seated structures range between ~4.5 and 8.2 km.

This analysis shows that:

1. the deep- and shallow-seated structures are characterised by well-separated wavelengths,
2. there is a large wavelength variability within the two different groups of structures.

3.2. Geological data

In the southernmost UMA, where the Neogene–Quaternary turbidite succession is almost completely missing, the compressional structures are exposed at the surface and can be effectively mapped.

Two major sets of compressional structures have been recognised in this region, whose geometry and kinematics have been described in the literature, using integrated surface geology data, seismic profiles and deep wells (e.g. Barchi et al., 1998):

- 'Umbria-Marche folds', detached within the Triassic evaporites (Burano Fm.; Martinis and Pieri, 1964), involving the whole carbonatic succession: they are box-shaped, NE verging anticlines, characterised by a wide, gently west dipping crestal zone, and steep, frequently overturned northeastern limbs, associated with outcropping or blind thrusts;
- 'Shallow imbricates', detached above a Cretaceous marly horizon (Marne a Fucoidi Fm.) or at the top of the carbonates, involving only the Paleogene marly succession and the thin overlying turbidites, where present. These are narrow, asymmetric folds, well exposed in the structurally low regions (i.e. synclinoria).

These two sets of structures can be easily recognised and distinguished in the geological maps throughout the region. We focus on the NW sector of the UMA, where a set of good quality and homogeneous maps (scale 1:10,000 and 1:50,000)

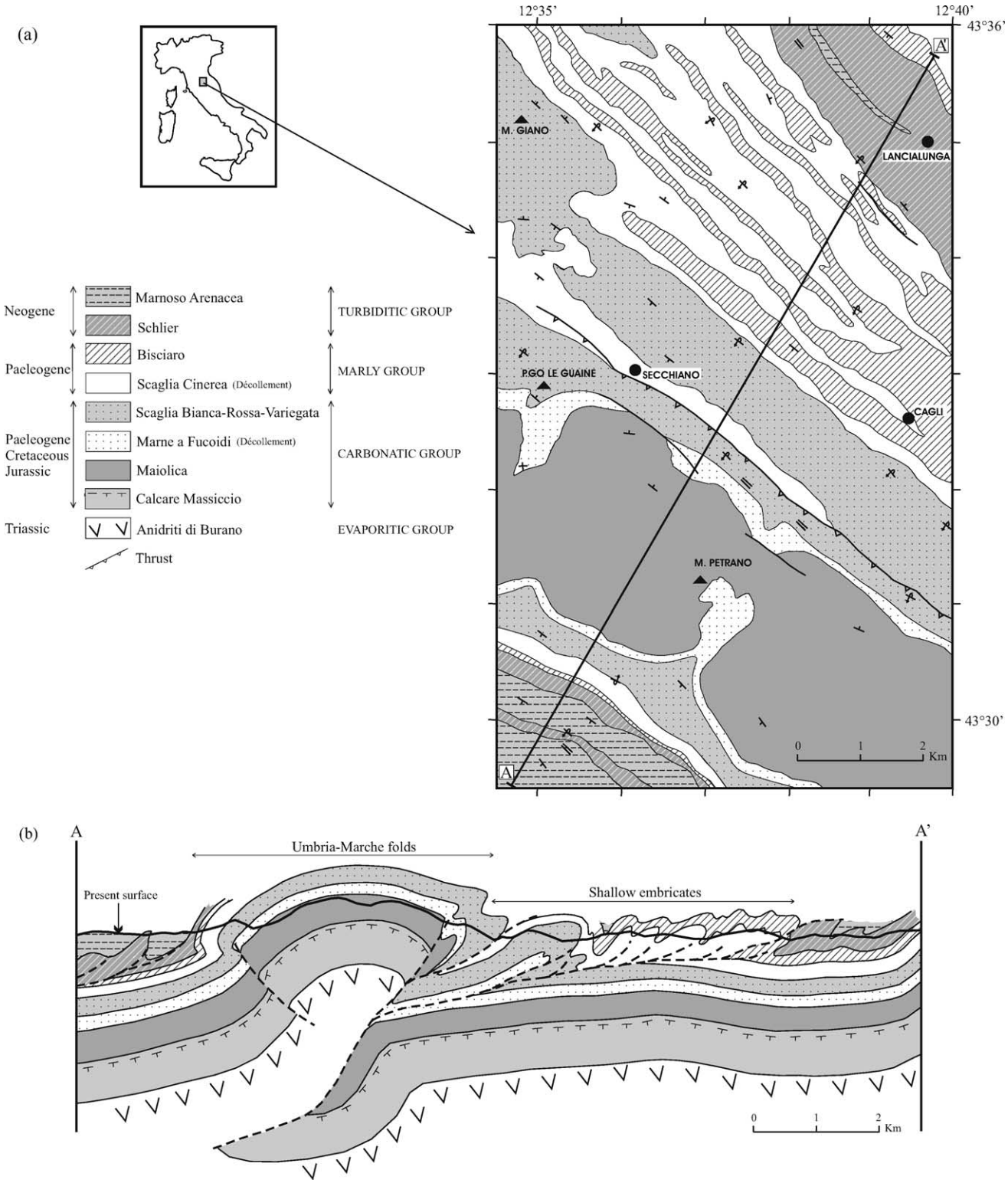

Fig. 4. (a) Schematic geological map of the Cagli area, located in the NW part of the UMA. (b) Geological section showing the presence of two sets of structures: the Umbria–Marche folds, involving the carbonatic succession, and the shallow imbricates, detached close to the top of the carbonates.

are available. Fig. 4 shows a geological cross-section, oriented SW–NE across the structural culmination of a northeastward verging box-fold (Mt. Petrano anticline). This fold involves the entire carbonates succession and is décolled along the underlying evaporites. Both the backlimb and the forelimb of the anticline are overturned and are cut by high angle thrusts. The Mt. Petrano anticline overthrusts towards NE a structurally low-elevated region, in the Cagli area. The geological section (Fig. 4b) shows that the major thrust that generates the Mt. Petrano anticline is décolled in the Triassic evaporites

and propagates eastward and upward in the stratigraphy into a flat trajectory in the marly horizons (Marne a Fucoidi Fm. and marly Group). It eventually splays out into a set of small, narrow, shallow-seated embricates. These embricates generate at their hanging-wall a complex pattern of asymmetric, NE verging, small-wavelength folds (Fig. 4b). This structural setting, the geometric and genetic relationships between deep-seated and shallow folds in particular, strictly resembles the Po Plain section, described in Section 3.1.

Using the geological maps, we constructed a set of 20, SW–NE oriented, closely spaced geological sections, orthogonal to the fold axes, parallel to the section of Fig. 4. The wavelengths of the larger and smaller folds were measured along the whole set of geological cross-sections. The results of this analysis show mean values of about 5 and 1.4 km for the larger ('Umbria-Marche folds') and smaller ('shallow embricates') structures, respectively (Fig. 5).

It is evident that these values are significantly lower than those obtained for the corresponding structures, buried below the Po Plain region (25 and 6 km, respectively). The stratigraphic position and lithology of the major décollement levels is the same in the UMA and below the PP. Therefore, the different wavelengths of the corresponding structures, which are about 4–5 times larger in the PP than in the UMA, is attributed to the presence of the thick clastic wedge, covering the compressional structures of the PP, inducing a greater décollement depth and a significantly greater thickness of the layers involved in the deformation. This is particularly evident for the shallow structures, since the Tertiary turbidites are almost completely missing in the UMA, where the shallow structures involve only the relatively thin (up to 500 m), Paleogene Marly Group.

4. Analogue models

4.1. Model setup

In the previous paragraph, we have seen how both PP and UMA are characterised by the presence of two major décollements, generating two different sets of structures. In order to better understand the geometrical and kinematic implications of this setting in the evolution of a thrust belt, we produced a set of seven sand-box models, scaled to the NA stratigraphy. Each model consisted of two horizontal weak horizons, at two different stratigraphic levels: one of the weak horizons was located at the base of the model, and the other in the middle of the model. The weak horizons, simulating décollements, consisted of glass micro-beads, whereas the competent rocks (carbonates and turbidites) were simulated by quartz sand (Fig. 2b).

Several parameters such as: dimensions, thickness and total bulk shortening were changed in the models. The width of the box in which the models were deformed was fixed to a constant 30 cm, the length of the box changed from 45 to 60 cm, while the model thickness ranged between 1.95 and 3.3 cm (Table 1). In order to obtain a comparable deformation in all the models,

(a)

Data source	Po Plain	
	$(\lambda)_l$	$(\lambda)_s$
Seismic Lines (this study)	22.5	8.2
	30.7	6.5
	33.2	6.1
	22.0	4.5
	$(\lambda)_l$	$(\lambda)_s$
Literature	15.8	7.5
	23.1	5.0
	33.0	
	21.2	
	18.7	
	28.7	

Data source	Umbria-Marche Apennines				
	$(\lambda)_l$		$(\lambda)_s$		
Geological maps 1:10.000	3.6		0.93		
	3.2		0.88		
	3.25		1.13		
			0.4		
	$(\lambda)_l$		$(\lambda)_s$		
Geological maps 1:50.000	3.56	5.685	1.875	2.302	0.72
	4.6	7.175	1.348	0.812	1.09
	4.734	5.375	1.215	0.828	1.435
	5.255	3.28	1.67	2.008	
	6.06	4.485	1.64	2.07	
	4.275	3.86	1.72	1.293	
	6.785	4.91	0.84	1.11	
	7.218	4.8	2.5	0.85	
	6.618		1.63	1.525	

Models						
$(\lambda)_l$				$(\lambda)_s$		
3.4	5.0	3.1	4.7	1.36	1.6	1.6
3.6	5.1	3.5	3.6	1.74	1.2	1.5
3.7	4.9	4.8	3.3	1.6	1.4	1.4
4.0	4.8	4.4	4.4	1.51	1.7	1.5
3.6	4.6	3.9	4.0	1.4	1.3	
3.5	3.1	3.8	4.2	1.1	1.8	
3.4	3.8	3.9	4.7	1.4	1.4	
3.3	4.1	3.9	4.2	1.3	1.6	
3.2	3.6	4.4	4.6	1.8	1.3	
3.7	3.7	4.6	4.2	1.7	1.6	
3.7	3.7	4.3	4.7	1.8	1.4	
3.5	3.6	4.8	4.8	1.4	1.3	
3.5	3.5	4.4	5.1	1.8	1.5	
3.8	3.8	4.3	4.5	2.3	1.5	
4.5	3.4	4.7	4.5	1.3	1.4	
4.9	3.2	5.0	4.3	1.5	1.1	
4.8	5.3	3.9	4.7	1.7	1.2	

(b)

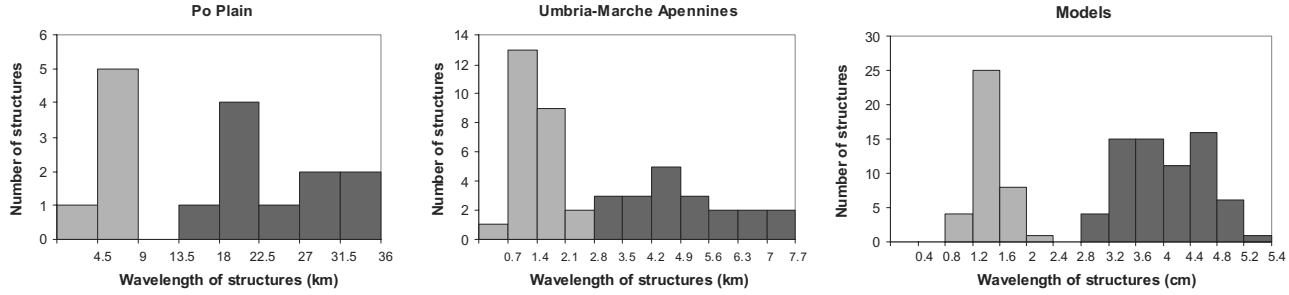

Fig. 5. (a) Measured values for the final wavelengths of the large, $(\lambda)_l$, and small, $(\lambda)_s$, structures of the Po Plain (PP), the Umbria–Marche Apennines (UMA) and the models. The values are expressed in kilometres for the PP and UMA, and in centimetres for the models. (b) Histograms of the final wavelengths of the structures. The bimodal shape of the histograms reflects the different values of the small (light grey) and large (dark grey) structure wavelengths.

Table 1
Parameters of the Po Plain (PPm) and Umbria–Marche (UMm) models

Parameter	PPm	UMm
Model width	30 cm	30 cm
Model length	60 cm	45 cm
Model thickness	3.3 cm	1.95 cm
Length ratio (l_m/l_n)	4×10^{-6}	4×10^{-6}
Shortening rate	2 mm/h	2 mm/h
Total shortening	45%	40%
Total time of shortening	14h25′	9h25′

the final bulk shortening was changed between 22.7 and 45%. The models were shortened above a planar, horizontal rigid basement at a constant velocity of 2 mm/h.

Horizontal layers of loose sand and glass beads were built by scraping. Coloured loose sand was put between different layers to act as strain markers. After constructing the layers, a square grid of loose sand was sieved onto the surface of the models to monitor the surface evolution. At fixed time intervals, measurements of: wedge taper angle, wedge elevation, distance of deformation front from the movable platen, thrust trajectory and distance between fixed points on top of the model were made and the model surface was photographed. At the end of the experiments, the models were covered with a layer of white loose sand to preserve the final configuration of the wedge, and wetted to make the sand cohesive for sectioning and photographing.

Below we discuss in detail the results of two of the seven models. One of the models is representative of the PP (labelled PPm) and the other one of the UMA (labelled UMm). These two models, present some similarities as well as differences (Table 1). They both simulate the effect of multiple décollements, are composed of similar materials and are subjected to a similar kinematic. However, they are scaled to two different regions of the NA, i.e. the PP and the UMA. In the PPm, syntectonic sediments ($\sim$0.5 cm) were added by sieving loose sand on the top of the model, at fixed intervals of shortening.

Although erosion and possible irregularities at basal boundaries have not been taken into account, the models simulate the evolution of a fold-thrust belt containing multiple décollements.

4.2. Scaling

The geometrical similarity between our models and nature was achieved by applying a precise length ratio to all model dimensions, where the length ratio was equal to 4×10^{-6}, implying that 4 mm in the model simulated 1 km in nature.

Kinematic similarity was approached by making the deformation sequence in the models similar to that in the NA. That is testified by the analogies between the structures detected on the seismic reflection profiles and geological data and those obtained in the models. In model PPm, kinematic similarity was reached by adding syntectonic sediments during the shortening.

Dynamic similarity was achieved using materials that enabled scaling intrinsic proprieties, such as the cohesion (τ_o) and the coefficient of internal friction (μ), between model and nature (see Cotton and Koyi, 2000 and references therein). Loose dry quartz sand and glass micro-beads were used to construct the models, because they represent appropriate materials to simulate the deformation occurring in the upper crustal rocks dominated by frictional behaviour (Mulugeta and Koyi, 1987; Gutscher et al., 1996). The loose sand utilised consists essentially of sub-angular quartz grains, with an angle of internal friction of $\phi=37°$. Due to its nearly perfect Mohr–Coulomb behaviour, this loose sand was used as an analogue of carbonatic and turbiditic rocks. To simulate the Marne a Fucoidi and the Triassic evaporites décollements glass micro-beads were used. This material consists of almost perfect spherical grains, and has an angle of internal friction of $\phi=25°$, consistently lower than the quartz sand.

4.3. Model results and comparison with NA

The most striking observation from the models is the presence of two sets of compressional structures, related to these two décollements: (1) large structures, detached above the deeper décollement and showing long wavelengths; (2) small structures, detached above the shallower décollement and characterised by short wavelengths.

During shortening, the layers were deformed and formed an imbricate wedge, whose main characteristic features were essentially governed by the larger structures. This wedge is composed mainly of foreland-vergent structures accreted in a piggy-back style. With progressive shortening, the early imbricate sheets steepened during the forward migration of the area of active deformation. As a consequence of the formation and the growth of a new imbricate, the pre-existing imbricates are back-rotated (i.e. their dip increased) and locked (Koyi and Schott, 2001).

Initial spacing between adjacent imbricates is small and increases with progressive build-up of the critical taper. The nucleation rate of new imbricates is high at the beginning of the deformation and decreases after the build-up of the critical taper. Progressive deformation of the models results in growth of the wedge, both in height and length, as new imbricates are accreted at its toe. The wedge grows faster at the beginning of the deformation, but its growth slows down as the critical taper is approached (Fig. 6). Such model behaviour is widely documented in the literature (Davis et al., 1983; Malavielle, 1984; Mulugeta and Koyi, 1987; Mulugeta, 1988; Colletta et al., 1991; Dixon and Liu, 1992; Marshak and Wilkerson, 1992).

Analysis of the models shows that deformation is mainly accommodated by the thrust sheets detached above the deeper décollement, whereas the small structures, decolling to the upper décollement, do not record a significant amount of shortening. A similar scenario occurs in the UMA, as shown in the balanced profile along the CROP03 section (Barchi et al.,

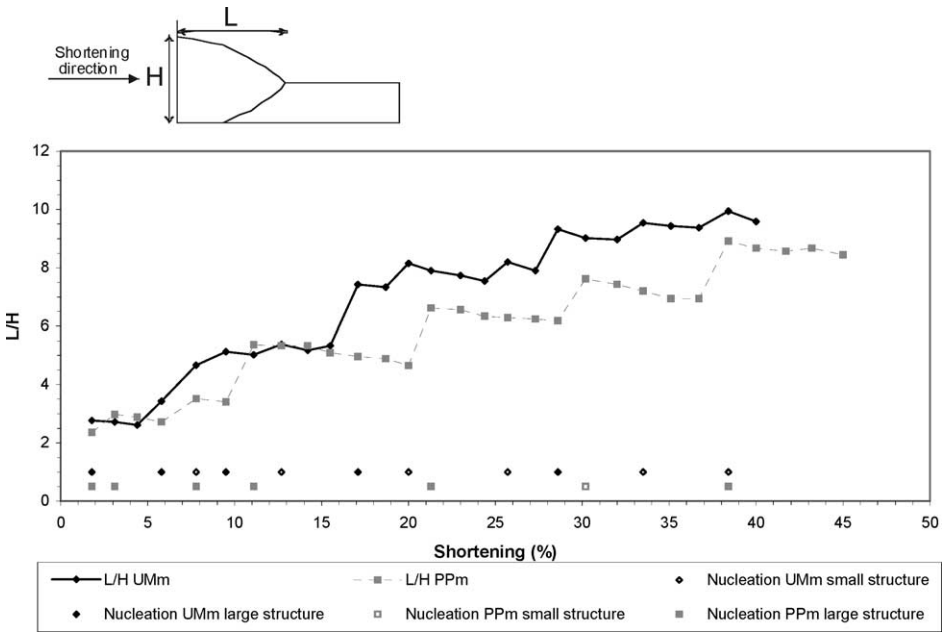

Fig. 6. Ratio of length (L) vs. height (H) of thrust wedge plotted against shortening (%). The plot indicates that a rapid increase of wedge length occurs at the nucleation of each new thrust sheet.

1998), and in many other studies on the UMA (e.g. Barchi, 1991; Ghisetti et al., 1993).

In the PP, the situation is quite different because the lack of information about the deeper geological setting prevents construction of balanced sections, including the Mesozoic units. This means that only the shortening due to the small structures can be actually evaluated, whilst the amount of shortening in the deeper part of the section cannot effectively be constrained (Castellarin et al., 1985; Perotti, 1991).

At the end of the deformation, in both PPm and UMm experiments, the layer of glass micro-beads, which acts as a weak horizon, accumulates in the core of the wedge. This is a common feature of all the models due to the mobility of the weaker material that tend to thicken in the anticline cores. A similar thickening is observed along the deep seismic profiles (e.g. Barchi et al., 1998) and documented by the anomalously high thickness of the Triassic evaporites (up to 3000 m) encountered in the deep wells drilled through the anticline cores (e.g. Burano well; Martinis and Pieri, 1964).

4.3.1. Structures development

In all the models, the presence of a shallower décollement level is responsible for the formation of a set of smaller structures. Below, we illustrate how these large and small structures are developed by describing in detail four longitudinal cross-sections of the PPm taken at different stages of deformation (through the glass sidewalls) of the models (Fig. 7). All these profiles were taken after the deposition of five layers of synkinematic sediments, added to the model by sieving sand on its top.

At bulk shortening of 23%, four closely spaced foreland-verging thrusts developed a wedge near the moveable platen followed by a box-fold representing the deformation front away from the platen (Fig. 7a). The older imbricates show similar geometry; their thrust surfaces are back-rotated (relative to the shortening direction) towards the hinterland and are characterised by a stratigraphic succession even more dislocated towards the bottom of the model.

With progressive shortening (32%) of the model (Fig. 7b), the forelimb of the box-fold develops a foreland verging thrust that propagates forward and upward until it over-thrusts the syntectonic sediments. The back-limb intensifies to form a back-thrust with a limited amount of displacement. The activation of the shallower décollement at this stage decouples the shallower layers from the deeper parts of the model. This shallow décollement is also responsible for the dislocation of the back-thrust in the back-limb of the most external anticline. At this stage, the upper part of the back-thrust is roughly subhorizontal, whereas its deeper part is dipping about 25° (Fig. 7b). The deformation is accommodated principally along the planar forward thrust. In the more external part of the model a new, smaller box-fold forms, above the shallower décollement.

At 35% of bulk shortening (Fig. 7c), the external box-fold, detached above the shallower décollement, amplifies. The fore-thrust of the large structure starts developing a homoclinal ramp trajectory (Fig. 7b), producing a ramp–flat–ramp geometry. The small structure forms in response to this displacement along the upper flat of the larger thrust. This flat is in fact both a hanging wall and footwall at the same time. The presence of this small structure testifies that the shallower and the deeper parts of the model accommodate the shortening in a disharmonic way. It is also possible to observe that during the shortening extensional structures form in the crest of the anticline: these extensional structures form due to fold crest collapse, producing characteristic crest grabens.

At 40% of bulk shortening (Fig. 7d) the small structure is not active any longer, and it is tilted and passively transported

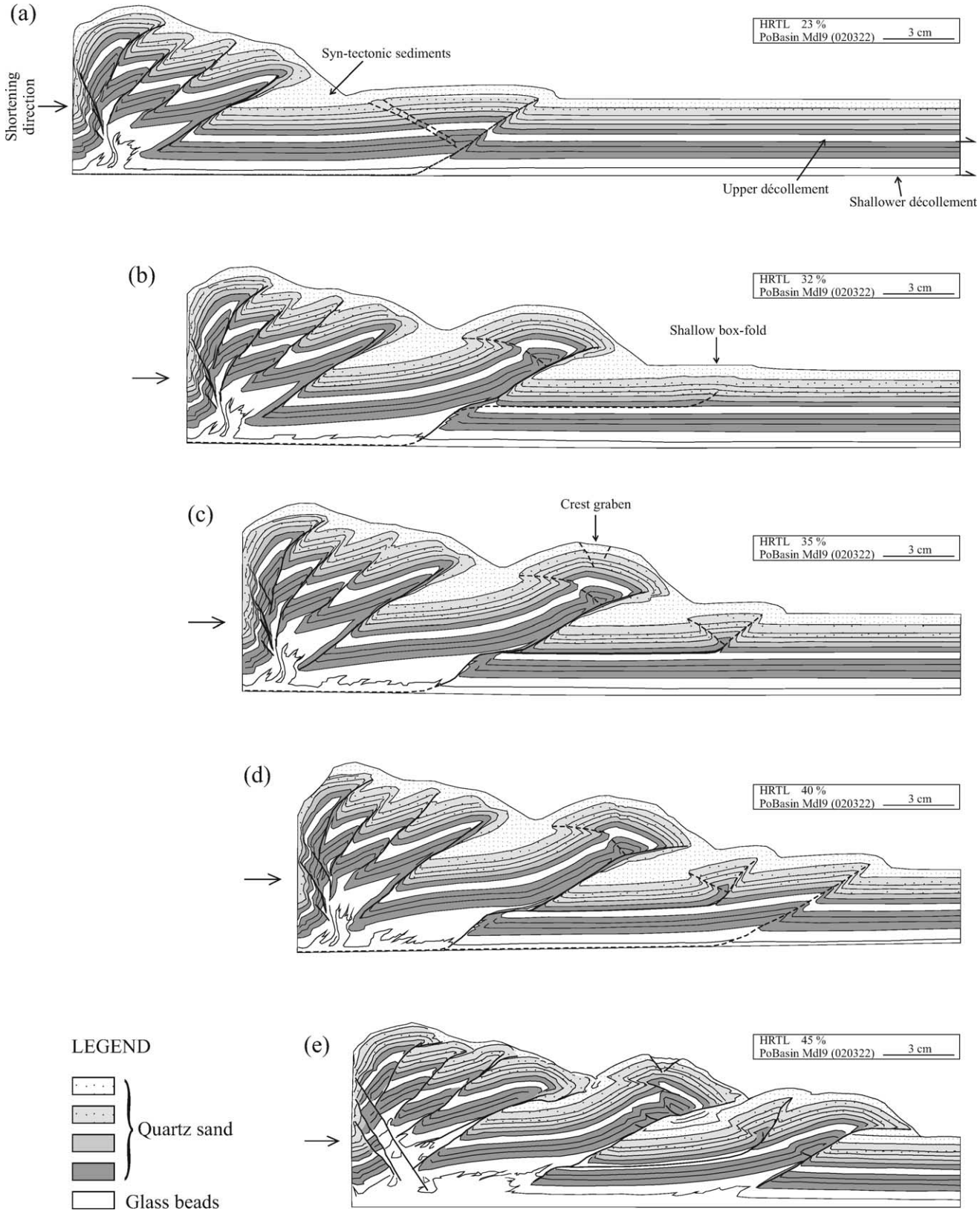

Fig. 7. Sequential line drawings of PPm at: (a) 23%, (b) 32%, (c) 35%, (d) 40% and (e) 45% shortening, respectively. The shortening was applied by moving a vertical rigid wall rightward. See text for description and discussion.

on the hanging wall of the new outermost structure, which is now the only active thrust.

5. Discussion

The models presented here show that vertical anisotropy (competence contrasts) generates structures with different characteristics that ultimately determine the deformation style of the entire thrust system.

Seismic data and results of analogue models are used to calculate the wavelength ratio between the different structures, in order to estimate the initial wavelength of the natural structures (otherwise unknown). Model results show that fold geometry evolves during the shortening in such a way that initial wavelength (when the thrust is active) is larger than the final wavelength (when the thrust is not active anymore). Initial and final wavelengths can be measured in the models, whilst in the natural systems only the final structural setting can be observed.

Using the results of the models, we estimate the initial wavelength (λ_i) of the large and small structures, $(\lambda_i)_l$ and $(\lambda_i)_s$, in nature, respectively. The final wavelength of the structures, both in nature and in models, $(\lambda_f)_l$ and $(\lambda_f)_s$, are known. The wavelengths referring to the large structures are marked with the letter l and those referring to the small structures with the letter s, whilst the wavelengths referring to nature are labelled with the letter N and those referring to the models with the letter M. If we assume that models are scaled to nature, the following equalities should hold:

- R_1: $[(\lambda_f)_s/(\lambda_f)_l]_M = [(\lambda_f)_s/(\lambda_f)_l]_N$;
- $(R_2)_l$: $[(\lambda_i/\lambda_f)_l]_M = [(\lambda_i/\lambda_f)_l]_N$ for the large structures
- $(R_2)_s$: $[(\lambda_i/\lambda_f)_s]_M = [(\lambda_i/\lambda_f)_s]_N$ for the small structures.

These conditions are called R_1, $(R_2)_l$ and $(R_2)_s$, respectively.

Checking to what extent the first condition is satisfied gives an idea about the degree of similarity between our models and their prototypes, while the conditions $(R_2)_l$ and $(R_2)_s$ can be used to calculate the unknown parameters $[(\lambda_i)_l]_N$ and $[(\lambda_i)_s]_N$, which represent the initial wavelength of the large and small natural structures, respectively.

In order to test condition R_1, we use model values, geological data and seismic reflection profiles. The results give the following numbers (Table 2):

- $(R_1)_M$: $[(\lambda_f)_s/(\lambda_f)_l]_M = 0.36$;
- $(R_1)_N$: $[(\lambda_f)_s/(\lambda_f)_l]_N = 0.25$ for the PP;
- $(R_1)_N$: $[(\lambda_f)_s/(\lambda_f)_l]_N = 0.27$ for the UMA.

The quite similar values of the ratio between the wavelengths of small and large structures $[(\lambda_f)_s/(\lambda_f)_l]_N$ of both PP and UMA (i.e. 0.25 and 0.27, respectively) suggest a similar mode of structural evolution for the entire NA.

Taking into account that some parameters, like erosion and lateral heterogeneity, are not included in our models, the difference between the model ratio value (0.36) and the nature average ratio value (0.26) is relatively small and we conclude that there is a good fit between our models and the PP and UMA.

For R_2, by substituting the opportune values to the parameters, we were able to determine the initial wavelength of the different structures in PP and UMA (Table 2):

1. $[(\lambda_i/\lambda_f)_l]_M = 1.24$. Given that $[(\lambda_i/\lambda_f)_l]_M \sim [(\lambda_i/\lambda_f)_l]_N$, by substituting the average value of $[(\lambda_f)_l]_N$ we obtain:
   - $[(\lambda_i)_l]_N = 30.85$ km for the PP structures;
   - $[(\lambda_i)_l]_N = 6.10$ km for the UMA structures
2. $[(\lambda_i/\lambda_f)_s]_M = 1.11$. Given $[(\lambda_i/\lambda_f)_s]_M = [(\lambda_i/\lambda_f)_s]_N$, considering the average value of $[(\lambda_f)_s]_N$ we calculate:
   - $[(\lambda_i)_s]_N = 6.95$ km for the PP structures;
   - $[(\lambda_i)_s]_N = 1.50$ km for the UMA structures.

This means, for instance, that a large structure in the PP with an initial λ of about 31 km, becomes about 25 km long, after the tectonic activity occurred in the area. A small structure of the UMA that is presently 2 km long may have started to form with an initial λ of 2.22 km.

Moreover, the similar value of the $(R_2)_l$ and $(R_2)_s$ conditions ($[(\lambda_i/\lambda_f)_l]_N = 1.24$ and $[(\lambda_i/\lambda_f)_s]_N = 1.11$, respectively) show that there is uniformity on the deformation pattern between the large and small structures of the NA.

The analysis of the wavelengths of the structures also illustrates how they are influenced by the depth of the décollement on which they are detached, confirming that the deeper the décollement, the larger the structures. With regard to this observation, we can also measure the ratio (K) between the final wavelength of the structures (λ_f) and the depth of the décollement (D) above which they are detached. Substituting the opportune values, we obtain (Table 2):

Table 2
Summary of geometrical characters of small and large folds. Wavelength values for the PP and the UMA are expressed in kilometres, whereas for the models in centimetres. The numbers in italics represent the estimated values for the initial wavelengths of the natural structures, calculated by using the R_2 condition. The numbers between brackets refer to the number of data utilised for the computation (see Fig. 5)

	PP		UMA		Models	
	Small	Large	Small	Large	Small	Large
λ_i	*6.95*	*30.85*	*1.50*	*6.10*	1.67 (3)	5.07 (4)
λ_f	6.26 (6)	24.88 (10)	1.35 (25)	4.92 (20)	1.50 (38)	4.1 (68)
$R_1 = [(\lambda_f)_s/(\lambda_f)_l]$	0.25		0.27		0.36	
$R_2 = [(\lambda_i/\lambda_f)]$					1.11	1.24
$K = \lambda_f/D$	1.2	2.4	1.3	1.2	2.3	2.1

- $(K_{PP})_l = 2.4$ and $(K_{PP})_s = 1.2$ for the large and small structures in PP, respectively;
- $(K_{UMA})_l = 1.2$ and $(K_{UMA})_s = 1.3$ for the large and small structures in the UMA;
- $(K_{mdls})_l = 2.1$ and $(K_{mdls})_s = 2.3$ for the model structures.

Except in the case of the PP, where the values of the ratio K for the two types of structures is quite different, in the other cases these values could be considered very similar. The difference between $(K_{PP})_l$ and $(K_{PP})_s$ is probably due to the lack of information about the actual depth of the décollement above which the PP large structures are detached, which can change in a wide range. Besides the unknown décollement depth, this can be due to mechanical proprieties of the rocks, thickness variations, style of deformation and timing of deformation, which are unknown.

6. Conclusions

We studied two different regions within the NA fold-and-thrust belt, using both seismic reflection profiles and surface geology data, to understand the effect of the presence of two different décollements on the structural pattern in the belt. We also built a set of sand-box models in the attempt to reproduce the final geometry and reconstruct the kinematics of thrusting in the NA fold-and-thrust belt.

Field and geophysical data and results of analogue models indicate that multiple décollements play a major role in the evolution of a thrust system, in response to the great importance of mechanical stratigraphy:

1. Different décollements produce different sets of structures, with different size, deformation history and importance. In the Northern Apennines, the presence of two major décollements induces the development of two sets of thrust related folds, which we named shallow- and deep-seated structures. These structures can easily be distinguished for their dimensions and relationships: shallower structures are generated by thrusts, splaying out from innermost, deep-seated structures.
2. The dimension of the structures greatly depends on the thickness of involved succession (i.e. depth of detachment);
   - deep-seated structures are systematically larger than shallow-seated structures;
   - in the Po Plain, where the carbonates are covered by a thick succession of Neogene turbidites (implying a greater depth of detachment), both deep- and shallow-seated structures are larger than in the Umbria–Marche Apennines where this thick succession is not preserved;
   - in the Po Plain, since the thickness of the Neogene turbidites is highly variable, the dimension of the structures is highly variable too, compared with the Umbria–Marche.
3. Model results suggest that the evolution of a wedge, containing multiple décollements, is essentially governed by the larger structures, detached at the deeper décollement, and that it follows the general rules of evolution of a Coulomb wedge, widely discussed by other authors. Model results confirm the geological and geophysical observations in the Northern Apennines: the deep-seated structures largely control syntectonic sedimentation (i.e. the location of the larger and deeper turbiditic basins) in the Po Plain, and accommodate most of the shortening of the Umbria–Marche Apennines. Both model results and natural examples indicate that the structure and evolution of a thrust belt remain dominated by the deep-seated structures, locally complicated by the shallow-seated structures.

Acknowledgements

Eni-E&P Division is acknowledged for having provided the seismic profiles: in particular, we wish to thank Dr Sergio Rogledi for the useful discussions and support in interpreting the seismic data. The authors thank G. Viola and F. Storti for their thorough and constructive reviews. Research founded by C.N.R. (CROP, resp. M.R. Barchi) and SAFE project (resp. G. Valensise, INGV). Hemin A. Koyi is funded by the Swedish Research Council (VR).

References

Alvarez, W., 1972. Rotation of the Corsica–Sardinia microplate. Nature Physical Science 235, 103–105.

Anzidei, M.P., Baldi, G., Casula, G., Galvani, A., Mantovani, E., Pesci, A., Riguzzi, F., Serpelloni, E., 2001. Insights into present-day crustal motion in the central Mediterranean area from GPS surveys. Geophysical Journal International 146 (1), 98–110.

Argnani, A., Ricci Lucchi, F., 2001. Tertiary silicoclastic turbidite system of the Northern Apennines. In: Vai, G.B., Martini, I.P. (Eds.), Anatomy of an Orogen: the Apennines and Adjacent Mediterranean Basins. Kluwer Academic Publishers, pp. 327–350.

Argnani, A., Bernini, M., Di Dio, G.M., Papani, G., Rogledi, S., 1997. Stratigraphic record of crustal-scale tectonics in the Quaternary of the Northern Apennines (Italy). Il Quaternario 10, 595–602.

Baker, D.M., Lillie, R.J., Yeats, R.S., Johnson, G.D., Yousuf, M., Hamid Zamin, A.S., 1988. Development of Himalayan frontal thrust zone: Salt Range, Pakistan. Geology 18, 3–7.

Baldacci, F., Elter, P., Giannini, E., Giglia, G., Lazzaretto, A., Nardi, R., Tongiorgi, M., 1967. Nuove osservazioni sul problema della falda toscana sulle interpretazioni dei flisch arenacei di tipo "Macigno" dell'Appennino Settentrionale. Memorie della Società Geologica Italiana 6, 218–244.

Bally, A.W., Burbi, L., Cooper, C., Ghelardoni, R., 1986. Balanced sections and seismic reflection profiles across the Central Apennines. Memorie della Società Geologica Italiana 35, 257–310.

Barchi, M.R., 1991. Integration of a seismic profile with surface and subsurface geology in a cross-section through the Umbria–Marche Apennines. Bollettino della Società Geologica Italiana 110, 469–479.

Barchi, M.R., De Feyeter, A., Magnani, M.B., Minelli, G., Pialli, G., Sotera, B.M., 1998. The structural style of the Umbria–Marche fold and thrust belt. Mememorie della Società Geologica Italiana 52, 557–578.

Barchi, M., Landuzzi, A., Minelli, G., Pialli, G., 2001. Outer northern Apennines. In: Vai, G.B., Martini, I.P. (Eds.), Anatomy of an Orogen: the Apennines and Adjacent Mediterranean Basins. Kluwer Academic Publishers, pp. 215–254.

Benedetti, L.C., Tapponier, P., Gaudemer, Y., Manighetti, I., Van der Woerd, J., 2003. Geomorphic evidence for an emergent active thrust along the edge of the Po Plain: the Broni–Stradella fault. Journal of Geophysical Research 108 (B5), 2238.

Berger, P., Johnson, A.M., 1980. First-order analysis of deformation of a thrust sheet moving over a ramp. Tectonophysics 70, 9–24.

Boccaletti, M., Coli, M., Eva, C., Ferrari, G., Giglia, G., Lazzaretto, A., Merlanti, F., Nicolich, R., Papani, G., Postpischl, D., 1985. Considerations on the seismotectonics of the Northern Apennines. Tectonophysics 117, 7–38.

Boyer, S.E., Elliot, D., 1982. Thrust systems. American Association of Petroleum Geologists Bulletin 66, 1196–1230.

Burrato, P., Ciucci, F., Valensise, G., 2003. An inventory of river anomalies in the Po Plain, Northern Italy: evidences for active blind thrust faulting. Annals of Geophysics 46/5, 865–882.

Cagnetti, V., Pasquale, V., Polinari, S., 1978. Fault-plane solutions and stress regime in Italy and adjacent regions. Tectonophysics 46, 239–250.

Castellarin, A., 2001. Alps–Apennines and Po Plain-frontal Apennines relations. In: Vai, G.B., Martini, I.P. (Eds.), Anatomy of an Orogen: the Apennines and Adjacent Mediterranean Basins. Kluwer Academic Publishers, pp. 177–196.

Castellarin, A., Eva, C., Giglia, G., Vai, G.B., 1985. Analisi strutturale del fronte appenninico padano. Giornale di Geologia 47/1–2 (3), 47–75.

Cello, G., Nur, A., 1988. Emplacement of foreland thrust system. Tectonics 7, 261–271.

Centamore, E., Deiana, G., Micarelli, A., Potetti, M., 1986. Il Trias-Paleogene delle Marche. In: Centamore, E., Deiana, G. (Eds.), La Geologia delle Marche Studi Geologici Camerti, Special Volume, pp. 9–27.

Channel, J.E.T., D'Argenio, B., Horwath, F., 1979. Adria, the African promontory. Mesozoic Mediterranean paleogeography. Earth Science Review 15, 213–292.

Chester, J.S., Logan, J.M., Spang, J.H., 1991. Influence of layering and boundary conditions on fault-bend and fault-propagation folding. Geological Society of American Bulletin 103, 1059–1072.

Cobbold, P.R., Rossello, E., Vendeville, B., 1989. Some experiments on interacting sedimentation and deformation above salt horizons. Bulletin de la Société Géologique de France 3, 453–460.

Colletta, B., Letouzey, J., Pinedo, R., Ballard, J.F., Balé, P., 1991. Computerized X-ray tomography analysis of sandbox models: examples of thin-skinned thrust system. Geology 19, 1063–1067.

Costa, E., Vendeville, B.C., 2002. Experimental insight on the geometry and kinematics of fold-and-thrust belts above weak, viscous evaporitic décollement. Journal of Structural Geology 24, 1729–1739.

Cotton, J.T., Koyi, H.A., 2000. Modeling of thrust fronts above ductile and frictional detachments: application to structures in the Salt Range and Potwar Plateau, Pakistan. Geological Society of American Bulletin 112, 351–363.

Cresta, S., Monechi, S., Parisi, G. (Eds.), 1989. Stratigrafia del Mesozoico e Cenozoico nell'area umbro-marchigiana. Itinerari geologici sull'Appennino umbro-marchigiano (Italia) Memorie Descrittive della Carta Geologica d'Italia, 39, pp. 1–182.

Dahlstrom, C.D.A., 1970. Structural geology in the eastern margin of the Canadian Rocky Mountains. Canadian Petroleum Geology Bulletin 18, 332–406.

Davis, D.M., Engelder, T., 1985. The role of salt in fold-and-thrust belts. Tectonophysics 119, 67–88.

Davis, D.M., Suppe, J., Dahlen, F.A., 1983. Mechanism of fold-and-thrust belts and accrectionary wedges. Journal of Geophysical Research 88, 1153–1172.

De Feyter, A.J., 1989. Gravity tectonics and sedimentation of the Montefeltro, Italy. Geologica Ultraiectina 35, 168.

Decandia, F.A., Giannini, E., 1977. Studi geologici nell'Appennino Umbro-marchigiano. 2) Le scaglie di copertura. Bollettino della Società Geologica Italiana 96, 723–734.

Di Bucci, D., Mazzoli, S., 2002. Active tectonics of the Northern Apennines and Adria geodynamics: new data and a discussion. Journal of Geodynamics 34, 687–707.

Dixon, J.M., Liu, S., 1992. Centrifuge modelling of the propagation of thrust faults. In: McClay, K.R. (Ed.), Thrust Tectonics. Chapman & Hall, London, pp. 53–69.

Doglioni, C., Prosser, G., 1997. Fold uplift versus regional subsidence and sedimentation rate. Marine and Petroleum Geology 14, 179–190.

Dondi, L., Mostardini, F., Rizzini, A., 1982. Evoluzione sedimentaria e paleogeografica della Pianura Paadana. In: Cremonini, G., Ricci Lucchi, F. (Eds.), Guida della geologia del margine appenninico-padano. Società Geologica Italiana, Guide Geologiche Regionali, pp. 47–58.

Eisenstadt, G., De Paor, D.G., 1987. Alternative model of thrust-fault propagation. Geology 15, 630–633.

Elliott, D., 1976. The energy balance and the deformation mechanisms of thrust sheets. Philosophical Transactions Royal Society of London A282, 289–312.

Elter, P., Giglia, G., Tongiorgi, M., Trevisan, L., 1975. Tensional and compressional areas in the recent (Tortonian to Present) evolution of north Apennines. Bollettino di Geofisica Teorica Applicata 17, 3–18.

Fermor, P.R., Moffat, I.W., 1992. Tectonics and structures of the Western Canada Foreland Basin. In: Macqueen, R.W., Leckie, D.A. (Eds.), Foreland Basins and Fold Belt. American Association of Petroleum Geologists Memoir, 55, pp. 81–105.

Fischer, M.P., Woodward, N.B., 1992. The geometric evolution of foreland thrust systems. In: McClay, K.R. (Ed.), Thrust Tectonics. Chapman & Hall, London, pp. 181–189.

Frepoli, A., Amato, A., 1997. Contemporaneous extension and compression in the Northern Apennines from earthquakes fault-plane solutions. Geophysical Journal of International 129, 368–388.

Gasparini, C., Iannacone, G., Scarpa, R., 1985. Fault-plane solutions and seismicity of the Italian Peninsula. Tectonophysics 117, 59–78.

Ghisetti, F., Barchi, M., Bally, A.W., Moretti, I., Vezzani, L., 1993. Conflicting Balanced Structural Sections Across the Central Apennine (Italy): Problems and Implications. In: Spencer, A.M. (Ed.), Generation, Accumulation and Production of Europe's Hydrocarbons III. Special Publication of the European Association of Petroleum Geoscientists, 3, pp. 219–231.

Grandinetti, F., Marcelli, C., Ferrara, E., Barchi, M.R., 2000. Modelli di evoluzione cinematica per un'anticlinale umbro-marchigiana. Bollettino della Società Geologica Italiana 119, 541–552.

Grelaud, S., Nalpas, T., Vergés, J., Karpuz, R., 2002. Role of décollement levels in thrust systems: field examples and analogue modelling. Bollettino di Geofisica teorica ed applicata 42 N.1/2 supplement, 178–180.

Gutscher, M., Kukowski, N., Malavielle, J., Lallemand, S., 1996. Cyclical behavior of thrust wedges: insights from high basal friction sandbox experiments. Geology 24, 135–138.

Koopman, A., 1983. Detachment tectonics in the Central Apennines, Italy. Geologica Ultraiectina 30, 155.

Koyi, H.A., Cotton, J., 2004. Experimental insights on the geometry and kinematics of fold-and-thrust belts above weak, viscous evaporitic décollement; a discussion. Journal of Structural Geology 26, 2139–2143.

Koyi, H.A., Schott, B., 2001. Stress estimations from fault geometries applied to sand-box and natural accrectionary wedges. Geophysical Research Letters 28 (6), 1087–1090.

Koyi, H.A., Sans, M., Teixell, A., Cotton J., Zeyen, H., 2003. The significance of penetrative strain in contractional areas. In: McClay, K.R. (Ed.), Thrust Tectonics and Petroleum Systems. American Association of Petroleum Geologists Memoir, vol. 82, p. 207–222.

Lavecchia, G., Minelli, G., Pialli, G., 1987. Contractional and extensional tectonics along the cross-section Lake Trasimeno-Pesaro (Central Italy). In: Boriani, A., Bonafede, M., Piccardo, G.B., Vai, G.B. (Eds.), The Lithosphere in Italy: Advances in Earth Sciences Research. Accademia Nazionale dei Lincei, Roma, pp. 177–194.

Lavecchia, G., Boncio, P., Creati, N., Brozzetti, F., 2004. Stile strutturale, stato termico-meccanico e significato sismogenetico del thrust Adriatico: dati e spunti da una revisione del profilo CROP 03 integrata con l'analisi di dati sismologici. Bollettino della Società Geologica Italiana 123, 111–125.

Letouzey, J., Colletta, B., Vially, R., Chermette, J.C., 1995. Evolution of salt-related structures in compressional settings. In: Jackson, M.P.A., Roberts, D.G., Snelson, S. (Eds.), Salt Tectonics: A Global Perspective. American Association of Petroleum Geologists Memoir, 65, pp. 41–60.

Leturmy, P., Mugnier, J.L., Vinour, P., Baby, P., Colletta, B., Chabron, E., 2000. Piggyback basin development above a thin-skinned thrust belt with two detachment levels as a function of interactions between tectonics and superficial mass transfer: the case of the Subandean Zone (Bolivia). Tectonophysics 320, 45–67.

Malavielle, J., 1984. Modélisation experimentale des chevauchements imriquées: Applications aux chaines de montagnes. Bulletin de la Société Géologique de France 7, 129–138.

Mariucci, M.T., Amato, A., Montone, P., 1999. Recent tectonic evolution and present stress in the Northern Apennines. Tectonics 18, 108–118.

Marshak, S., Wilkerson, M.S., 1992. Effect of overburden thickness on thrust belt geometry and development. Tectonics 11 (3), 560–566.

Martinis, B., Pieri, M., 1964. Alcune notizie sulla formazione evaporitica dell'Italia centrale e meridionale. Memorie della Società Geologica Italiana 4, 649–678.

Mitra, S., 1986. Duplex structures and imbricate thrust systems: geometry, structural position and hydrocarbon potential. American Association of Petroleum Geologists Bulletin 70, 1087–1112.

Mulugeta, G., 1988. Modelling the geometry of Coulomb thrust wedges. Journal of Structural Geology 10 (8), 847–859.

Mulugeta, G., Koyi, H.A., 1987. Three-dimensional geometry and kinematics of experimental piggyback thrusting. Geology 15, 1052–1056.

Ori, G.G., Roveri, M., Vannoni, F., 1986. Plio-Pleistocene sedimentation in the Apenninnic-Adriatic foredeep (Central Adriatic Sea, Italy). In: Allen, P.A., Homewood, P. (Eds.), IAS Special Publication 8, Foreland Basins, pp. 183–198.

Ori, G.G., Serafini, G., Visentin, C., Ricci Lucchi, F., Casnedi, R., Colalongo, M.L., Mosna, S., 1991. The Pliocene–Pleistocene Adriatic Foredeep (Marche and Abruzzo, Italy): an Integrated Approach to Surface and Subsurface Geology 1991. 3rd European Association Petroleum Geologists, Conference Field Trip Guidebook, Florence, 85pp.

Passeri, L. (Ed.), 1994. Appennino Umbro–Marchigiano. Guide Geologiche Regionali 7. Società Geologica Italiana, BE-MA, Milano. 301pp.

Pauselli, C., Marchesi, R., Barchi, M.R., 2002. Seismic image of the compressional and extensional structures in the Gubbio area (Umbria–Pre Apennines). Bollettino della Società Geologica Italiana, Special Volume 1, 263–272.

Perotti, C.R., 1991. Osservazioni sull'assetto strutturale del versante padano dell'Appennino nord-occidentale. Atti Ticinensi Scienze della Terra 34, 11–22.

Pialli, G., Barchi, M.R., Minelli, G. (Eds.), 1998. Results of the Crop03 Deep Seismic Reflection Profile. Memorie della Società Geologica Italiana 52.

Pieri, M., 1983. Three seismic profiles through the Po Plain. In: Bally, A.W. (Ed.), Seismic Expression of Structural Styles. American Association of Petroleum Geologists, Studies in Geology, 15(3.4.1), pp. 8–26.

Pieri, M., Groppi, G., 1981. Subsurface geological structure of the Po Plain (Italy). Pubblicazione del Progetto Finalizzato Geodinamica C.N.R. 414, 1–23.

Reutter, K.J., Giese, P., Closs, H., 1980. Lithospheric split in the descending plate: observations from the Northern Apennines. Tectonophysics 64, T1–T9.

Ricci Lucchi, F., Colalongo, M.L., Cremonini, G., Gasperi, G., Iaccarino, S., Papani, G., Raffi, S., Rio, D., 1982. Evoluzione sedimentaria e paleogeografica nel margine appenninico. In: Cremonini, G., Ricci Lucchi, F. (Eds.), Guida alla geologia del margine appenninico-padano. Società Geologica Italiana, Guide Geologiche Regionali, pp. 17–46.

Rizzini, A., Dondi, L., 1979. Messinian evolution of the Po Basin and its economic implications (hydrocarbons). Paleogeography, Paleoclimatology, Paleoecology 29, 41–74.

Sage, L., Mosconi, A., Moretti, I., Riva, E., Roure, F., 1991. Cross section balancing in the central Apennines; an application of LOCACE. American Association Petroleum Geologists Bulletin 75, 832–844.

Sans, M., Vergés, J., 1995. Fold development related to contractional salt tectonics: Southeastern Pyrenean thrust front, Spain. In: Jackson, M.P.A., Roberts, D.G., Snelson, S. (Eds.), Salt Tectonics: A Global Perspective. American Association of Petroleum Geologists Memoir, 65, pp. 369–378.

Selvaggi, G., Ferulano, F., Di Bona, M., Frepoli, A., Azzarra, R., Basili, A., Chiarabba, C., Ciaccio, M.G., Di Luccio, F., Lucente, F.P., Margheriti, L., 2001. The Mw 5.4 Reggio Emilia 1996 earthquakes: active compressional tectonics in the Po Plain, Italy. Geophysical Journal International 144, 1–13.

Sorgi, C., Deffontaines, B., Hippolyte, J.C., Cadet, J.P., 1998. An integrated analysis of transverse structures in the Northern Apennines, Italy. Geomorphology 25, 193–206.

Teixell, A., 1996. The Ansò transect of the southern Pyrenees: basement and cover thrust geometries. Journal of Geological Society of London 153, 301–310.

Teixell, A., Koyi, H.A., 2003. Experimental and field study of the effects of lithological contrasts on thrust-related deformation. Tectonics 22, 1054–1073.

Turrini, C., Ravaglia, A., Perotti, C.R., 2001. Compressional structures in a multi-layered mechanical stratigraphy: insights from sandbox modeling with three dimensional variation in basal geometry and friction. In: Koyi, H.A., Mancktelow, N.S. (Eds.), Tectonic Modeling: a Volume in Honour of Hans Ramberg. Geological Society of America Memoir, 193, pp. 153–178.